Sensors and Materials, Vol. 37, No. 5 (2025) 1959–1967
MYU Tokyo

S & M 4033

High-temperature Operation Characteristics of Diamond Radiation Detectors

Masakatsu Tsubota,[1] Takehiro Shimaoka,[1] Yuto Akashi,[1*] Shintaro Hirano,[1]
Akiyoshi Chayahara,[2,3] Yukako Kato,[2] Hitoshi Umezawa,[2]
Hideyuki Watanabe,[2] Yoshiaki Mokuno,[2] and Junichi H. Kaneko[1]

[1]Graduate School of Engineering, Hokkaido University, Kita 13 Nishi 8, Kita-ku, Sapporo 060-8628, Japan
[2]Research Institute for Ubiquitous Energy Devices, National Institute of Advanced Industrial Science and Technology, 1-8-31, Midorigaoka, Ikeda, Osaka 563-8577, Japan
[3]Research Institute for Electronics and Photonics, National Institute of Advanced Industrial Science and Technology, 1-1-1 Higashi, Tsukuba, Ibaraki 305-8562, Japan

(Received January 8, 2025; accepted May 1, 2025)

Keywords: charge collection efficiency, diamond detector, high-temperature operation, $\mu\tau$ product, single-crystal diamond

The high-temperature operation of a diamond radiation detector was demonstrated with charge collection efficiency at temperatures up to 500 °C. The detector operated steadily even at high temperatures because a guard ring suppressed the increase in leakage current. Charge transport properties were almost identical to those obtained at room temperature. The $\mu\tau$ product of the hole and energy resolution of electrons improved at high temperatures.

1. Introduction

Diamond has unique properties such as high radiation resistance, temperature tolerance, body equivalence, and high responsiveness. Advances in synthesis techniques have led to the development of radiation detectors with applications in high-energy physics, nuclear fusion, medical irradiation, and space environments. In particular, diamond has a wide band gap of 5.47 eV. Therefore, it is expected to operate at temperatures higher than those of other wide-band-gap semiconductors such as SiC (4H, 6H, and 3C) and GaN (3.26 eV for 4H, 2.93 eV for 6H, and 2.23 and 3.39 eV for 3C). Typical applications of detectors in high-temperature and high-dose environments include attempts to measure plasma ion temperatures on the basis of DT neutron measurements in fusion[(1–3)] and thermal neutron measurements,[(4,5)] with the former energy measurements at 300 °C having been reported.[(6)] In the case of the nuclear reactor core atmosphere monitor, which is required in the event of a severe nuclear reactor accident, the maximum temperature for the γ-ray dosimeter is 300 °C, and it should operate for one week. In addition, the γ-ray detector for the water level meter in the pressure vessel, which is being considered for installation in the nuclear reactor containment vessel, is expected to be used at

*Corresponding author: e-mail: tsrdcws4698@eis.hokudai.ac.jp
https://doi.org/10.18494/SAM5528

ISSN 0914-4935
https://myukk.org/

temperatures between 300 and 500 °C. In this study, we investigated the operation of radiation detectors at high temperatures of up to 500 °C.

The forbidden bandwidth of diamond is large at 5.47 eV, and the energy levels attributable to structural defects and/or others observed in cathode luminescence measurements often do not cause significant interference with detector operation at room temperature. However, as the operating temperature increases, the leakage current increases with energy levels, and the detector stops working.[7]

With 4H-SiC, an energy resolution of 1.6% was reported in response to 5.5 MeV α-particle irradiation at 300 °C.[8] At higher temperatures, the resolution degraded. Then, the full width at half maximum increased to about 10 times at 500 °C compared with that at room temperature, although the 4H-SiC detector remained operational.[9] There are only few reports of radiation detector of GaN in high-temperature operation. The radiation detector of GaN operated below 300 °C was reported.[10] A THz detector operated at 200 °C was also reported.[11]

Kozlov*et al.* reported a diamond detector made of a natural type-IIa single crystal.[12] For synthetic crystals, a diamond detector made of a type-IIa single crystal synthesized by a high-pressure/high-temperature (HP/HT) process[13] and that made of a type-IIa single crystal synthesized by microwave plasma chemical vapor deposition (CVD)[7] have been reported. To date, energy spectral measurements have been performed up to 300 °C.[14] Further measurements were made up to 500 °C, and it was reported that the amount of charge collected decreased by about 30% above 250 °C.[15]

For this study, we investigated the characteristics of single-crystal CVD diamond detectors synthesized at temperatures up to 500 °C. We prepared a diamond synthesized by Hokkaido University (HU) and that purchased from Element Six Ltd. (E6); then, we fabricated detectors by the same process. The cathodoluminescence spectra (CL) of the crystals were evaluated. We measured the charge distribution induced by 5.486 MeV α-particle irradiation from an ^{241}Am source to ascertain the current state of the art of diamond detectors. The $\mu\tau$ product was evaluated.

2. Experimental Details

Diamond was synthesized on a type-IIa single-crystal diamond substrate by the HP/HT process developed by Sumitomo Electric Industries, Ltd.[16,17] under the following conditions: hydrogen and 0.2% methane mixed gases of 110 Torr pressure and substrate surface temperature of 900 °C. This type IIa single-crystal diamond substrate has excellent crystallinity with nitrogen impurities of around 1 ppm and a full width at half maximum of a few arcsec in the double crystal rocking curve. The homoepitaxial growth of single-crystal diamond was accomplished by microwave plasma CVD. The microwave plasma reactor (AX5250; Seki Technotron Corp.) produced plasmas at high power densities. To ensure reproducibility and the reuse of the expensive substrate, we used the lift-off process.[18–20] After the separation of the growth layer by electrolytic etching, the back surface of the substrate layer was irradiated with an ion beam to remove the remaining substrate. Figure 1 shows a diffraction interference microscopy image. The sample dimensions were 85 mm thickness and 5 × 5 mm^2 area. To deposit a guard ring electrode by photolithography, a crystal without roughness on the surface

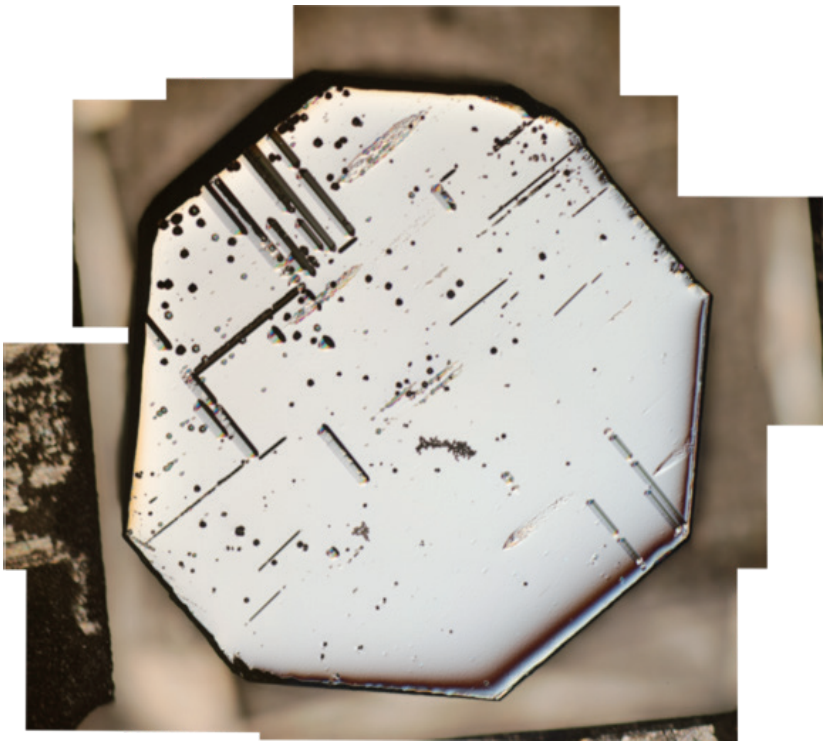

Fig. 1. (Color online) Diffraction interference microscopy image of diamond synthesized by the lift-off method.

was chosen. Details of the crystal synthesis and the detector performance at room temperature were presented by Shimaoka and coworkers.[21,22] The detector fabricated using the diamond synthesized under the condition described above has an energy resolution of 0.38% in response to 5.486 MeV α-particles. Furthermore, in 14 MeV neutron energy spectrum measurement, which is one application described above, the detector achieved an energy resolution of 0.8%.[23]

No impurities in HU and E6, which are electronics-grade single-crystal diamonds synthesized by CVD, were not detected below the measurement limit of secondary ion mass spectroscopy (SIMS). In particular, nitrogen was detected at less than part per billion order, which makes a deep level of 1.7 eV below the conduction band. Increased charge-up and leakage currents at high temperatures and in high-count-rate environments are most likely due to defects. Figure 2 shows the cathodoluminescence spectra obtained from typical HU diamond and E6 diamond used for the application of the radiation detector. In the HU diamond with a reduced growth rate, a free-exciton recombination emission was observed only at 235 nm, corresponding to a band gap, which typically reflects the crystalline perfection of diamond. The harmonic wave of recombination luminescence at 235 nm located at 470 and 705 nm. On the other hand, in the diamond produced using E6, other emissions were observed at around 400–500 and 500–700 nm.

After HU diamond synthesis, the surface state was changed by the dichromate treatment from hydrogen-terminated to oxygen-terminated to decrease the surface conductivity. Next, we fabricated the diamond radiation detector by attaching metal electrodes. The Ti/Pt electrode was attached to the as-grown surface of these CVD single-crystal diamonds by vapor deposition. A

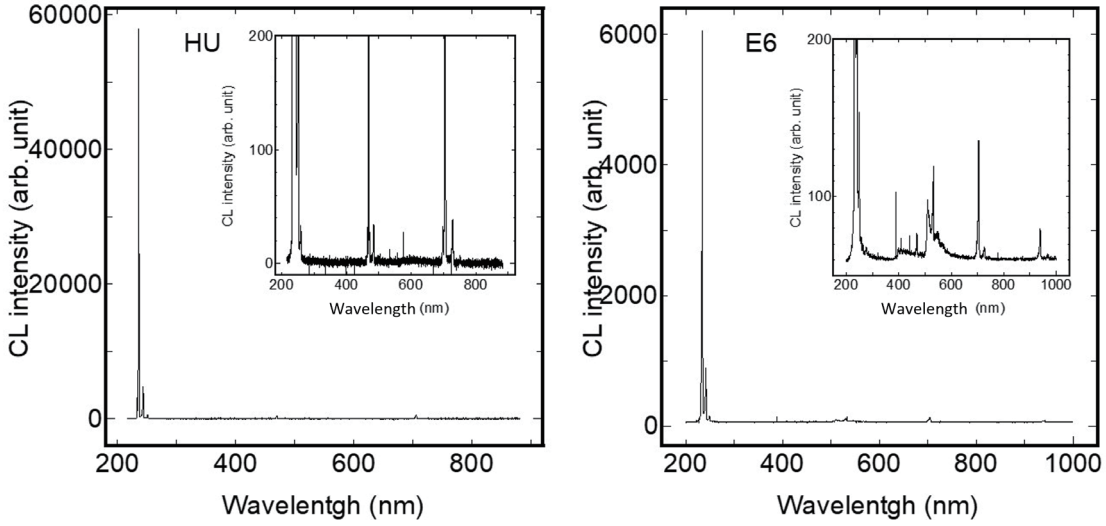

(a) (b)

Fig. 2. Cathodoluminescence spectra of (a) HU diamond and (b) E6 diamond.

Pt electrode was attached to the other side. The Ti and Pt thicknesses were both 50 nm. The Ti/Pt electrode was a center electrode of 2.5 mm radius with a guard ring of 4.0 mm radius and 0.3 mm width. The TiC layer was fabricated at the interface with diamond by vacuum heating at 400 °C for 30 min. The Pt electrode did not carbonize at around 600 °C. Therefore, it is regarded as a Schottky electrode.[24] The thickness and area of the E6 diamond, which was prepared for comparison, were 500 mm and 4 × 4 mm^2, respectively, and the electrode was the center electrode of 2.0 mm radius with a guard ring of 3.5 mm radius and 0.3 mm width.

Figure 3 shows the experimental setup used. A charge-sensitive preamplifier (142A; Ortec), a detector bias supply (428; Ortec), a spectroscopy amplifier (672; Ortec), and a multichannel analyzer (WE7562; Yokogawa Analytical Systems Inc.) were used. The diamond detector and the radiation source ^{241}Am were put in the vacuum chamber. α-Particles (5.486 MeV) from the ^{241}Am source impinged on the detector only within the TiC/Pt contact surface. The output signal was taken out through a microprobe. We used a source measurement unit (237; Keithley Instruments, Inc.) for leakage current–applied voltage (*I–V*) measurements. The measurements were performed in air. The main collected charge of the electron and hole was switched by changing the polarity of the applied voltage, as no significant difference in leakage current depending on the polarity of the applied voltage was found.

3. Results and Discussion

3.1 *I–V* characteristics

First, we measured the *I–V* characteristics by changing the temperature to evaluate rectification properties. Figure 4 shows the temperature dependence of *I–V* characteristics at room temperature (23 °C), 300, and 500 °C with and without a guard ring. One side was made into a Schottky electrode for suppressing leakage current, but no rectification characteristics

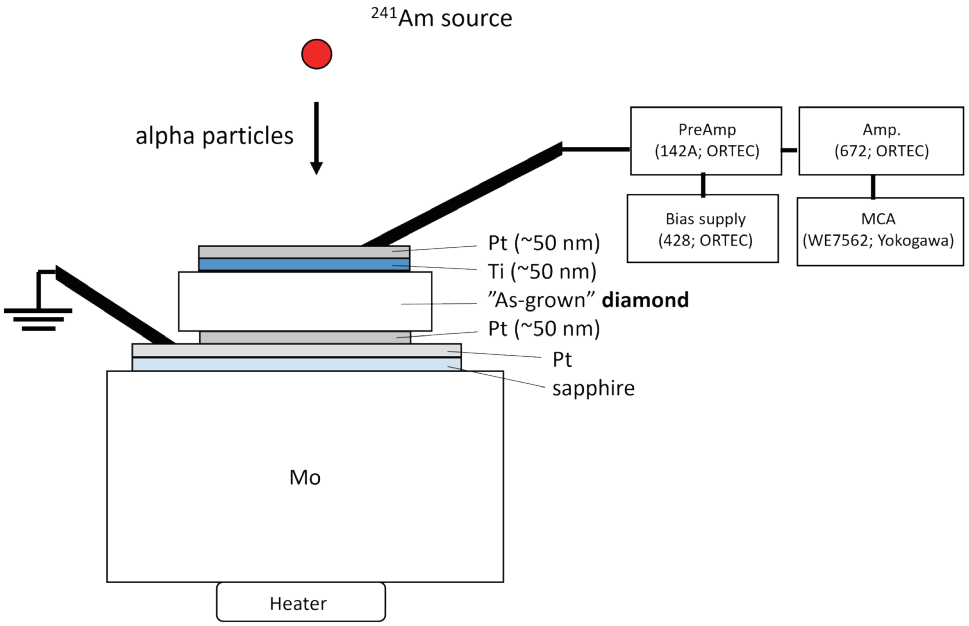

Fig. 3. (Color online) Experimental setup.

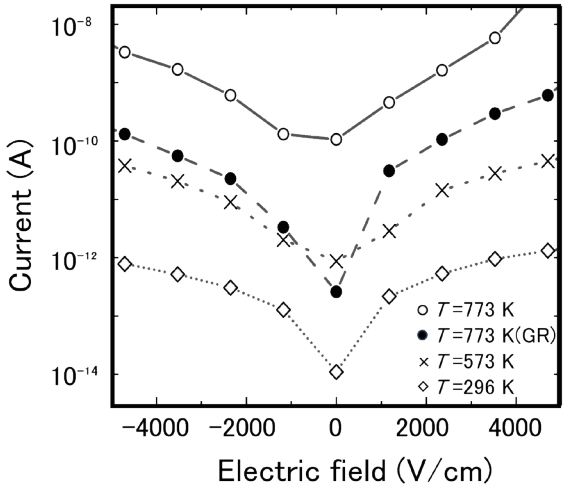

Fig. 4. *I–V* characteristics measured at different temperatures. The leakage current was reduced by attaching the guard ring (GR).

were observed. The HU diamond detector changed to an oxygen-terminated surface with a current flow of only less than 1 pA in an electric field of 2000 V/cm at room temperature, which was a sufficiently low current required for radiation measurement. The current increased to about 1 nA at 500 °C. The line GR in Fig. 4 shows the leakage current with a guard ring at 500 °C. Then, the current decreased to about 10 pm. Since a leakage current of about 100 pA at 2000 V/cm is not a practical problem, it is possible to reduce the surface leakage current only by the oxygen termination of diamond up to 300°C. The guard ring became effective at temperatures higher than 300 °C.

3.2 Temperature dependence of induced charge distribution

Next, we measured the charge distribution induced by 5.486 MeV α-particle irradiation while applying positive and negative biases. Figure 5 shows the temperature dependence of charge collection efficiency (CCE). The detectors were produced by the same process using (a) HU diamond and (b) E6 diamond. A silicon surface barrier detector was used for the calibration of CCE. The average energies for the hole–electron pair creation of silicon and the CVD diamond, namely, 3.62 and 13.1 eV,[12] respectively, were used for calculations. As a preliminary measurement, the peak channel of the Si semiconductor detector was determined, and then the CCE of the diamond detector was evaluated by comparing the average energies. Although the energy resolution became the reference because of the RF noise as a result of the measurements through the microprobe with no impedance matching, the resolutions of the hole and electron were 0.9 and 1.3%, respectively, at room temperature. With increasing temperature, however, the hole and electron resolutions increase to 0.6 and 0.8%, respectively. It is possible that the trapped charge was released by thermal excitation.

The peak position of CCE corresponding to the electron did not change, but it clearly improved in the case of the hole. Although the reason has not been determined, it must be clarified by the signal analysis of the preamplifier in the future. Because the heat tolerance limit of the ^{241}Am source has been reached by radiant heat, we did not measure it at temperatures higher than 500 °C in our experimental setup. At higher temperatures, the detector limit must be investigated.

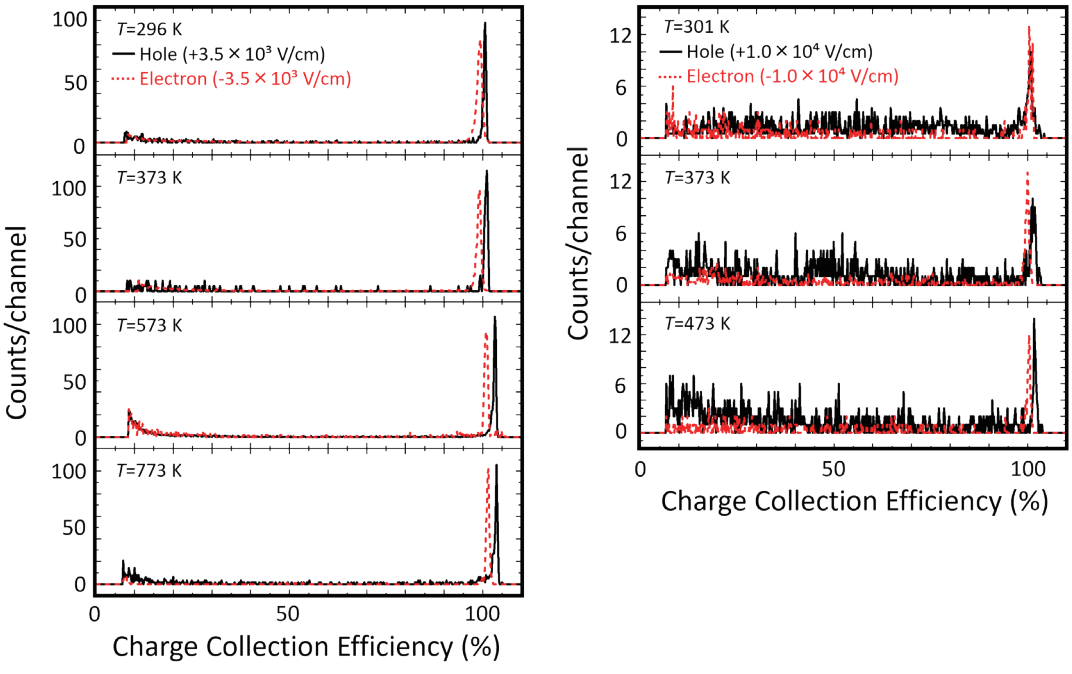

Fig. 5. (Color online) Temperature dependence of CCE using (a) HU diamond and (b) E6 diamond.

Figure 5(b) shows the CCE of the detector using E6 diamond. No CCE peak was observed at 220 °C. A diamond crystal for a detector operating at 300 °C exists, but we tried and failed to measure 10 samples at 60–220 °C because of the increasing leakage current.

In the case of the E6 sample, the peak disappeared at temperatures higher than 500 °C. CCE was obtained by comparing the α-ray peak positions of the surface barrier Si semiconductor detector (CU-1250-100; EG&G ORTEC) and the average electron–hole production energies of silicon (3.62 eV) and diamond (13.1 eV).[12]

3.3 Temperature dependence of mobility–lifetime products

Finally, the mobility–lifetime ($\mu\tau$) products were estimated using the electric field dependence of CCE, shown as charge transport properties. The $\mu\tau$ products were calculated using Heckt's equation[25] as

$$\frac{Q(E)}{Q_0} = \frac{\mu\tau E}{d}\left[1 - \exp\left(-\frac{d}{\mu\tau E}\right)\right], \tag{1}$$

where d represents the sample thickness, E denotes the electric field, Q_0 stands for the total charge, and $Q(E)$ expresses the CCE measurement. The electric fields were set to $\pm 3.5 \times 10^3$ and $\pm 1.0 \times 10^4$ V/cm at HU and E6, respectively, so that CCE saturates without causing dielectric breakdown.

Figure 6 shows the temperature dependence of $\mu\tau$ products determined using Hecht's equation as shown in the above equation related to the applied voltage and CCE peak position. Both the hole and electron values were about 10^{-5} cm^2/V, which was smaller than the average of HU diamond detectors. However, the value of the hole improved considerably with increasing temperature. Then, it reached 2×10^{-4} cm^2/V at 500 °C.

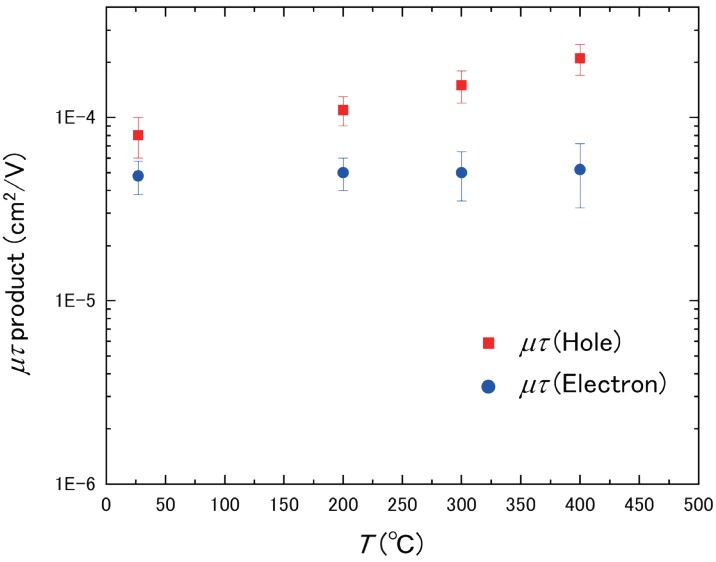

Fig. 6. (Color online) Temperature dependence of mobility–lifetime ($\mu\tau$) products.

As described above, a diamond with a smooth surface was chosen because the guard ring electrode was fabricated by photolithography. The crystals were synthesized in the outer edge region of the plasma where etching was limited. In this case, etching did not adequately remove areas of weak bonding and poor crystallinity. Therefore, the value of the $\mu\tau$ product could only be up to 10^{-5} cm^2/V.

4. Conclusion

A radiation detector made of diamond synthesized using hydrogen and 0.2% methane mixed gases was operated at 500 °C. The CCE and energy resolution of the hole and electron were almost identical to those at room temperature. The increase in leakage current, which was the problem of signal detection, might be reduced by the guard ring. A diamond diode operating even at 700 °C was reported.[26] The carbonization of the diamond–metal interface occurs at about 650 °C.[27] Therefore, the next objective is to confirm whether the detector operates at 700 °C. We expect to reduce the temperature rise of the α-particle source and improve the signal detection method in future work.

Acknowledgments

This paper includes some results obtained from studies under the project “Development of diamond electric devices for nuclear power reactors withstanding a severe accident” under the auspices of the Ministry of Education, Culture, Sports, Science, and Technology of Japan.

References

1 A. V. Krasilnikov, J. Kaneko, M. Isobe, F. Maekawa, and T. Nishitani: Rev. Sci. Instrum. **68** (1997) 1720. https://pubs.aip.org/aip/rsi/article/68/4/1720/148815/Fusion-Neutronic-Source-deuterium-tritium-neutron
2 G. J. Schmid, J. A. Koch, R. A. Lerche, and M. J. Moran: Nucl. Instrum. Methods Phys. Res., Sect A **527** (2004) 554. https://dialnet.unirioja.es/servlet/articulo?codigo=924520
3 C. Cazzaniga, M. Nocente, M. Rebai, M. Tardocchi, P. Calvani, G. Croci, L. Giacomelli, M. Girolami, E. Griesmayer, G. Grosso, M. Pillon, D. M. Trucchi, and G. Grini: Rev. Sci. Instrum. **85** (2014) 11E101. https://pubs.aip.org/aip/rsi/article/85/11/11E101/360371/A-diamond-based-neutron-spectrometer-for
4 R. Pilotti, M. Angelone, M. Marinelli, E. Milani, G. Verona-Rinati, C. Verona, G. Prestopino, R. M. Montereali, M. A. Vincenti, E. M. Schooneveld, A. Scherillo, and A. Pietropaolo: Appl. Phys. Lett. **116** (2016) 42001. https://iopscience.iop.org/article/10.1209/0295-5075/116/42001
5 M. Marinelli, E. Milani, G. Prestopino, M. Scoccia, A. Tucciarone, and G. Verona-Rinati: Appl. Phys. Lett. **89** (2006) 143509. https://pubs.aip.org/aip/apl/article/89/14/143509/332295/High-performance-Li6F-diamond-thermal-neutron
6 A. Kumar and A. Topkar: IEEE Trans. Nucl. Sci. **65** (2018) 630. https://ieeexplore.ieee.org/stamp/stamp.jsp?arnumber=8214276
7 M. Tsubota, J. H. Kaneko, D. Miyazaki, T. Shimaoka, K. Ueno, T. Tadokoro, A. Chayahara, H. Watanabe, Y. Kato, S, Shikata, and H. Kuwabara: Nucl. Instrum. Methods Phys. Res., Sect. A **789** (2015) 50. https://www.sciencedirect.com/science/article/pii/S0168900215004556
8 T. R. Garcia, A. Kumar, B. Reinke, T. E. Blue, and W. Windl: Appl. Phys. Lett. **103** (2013) 152108. https://pubs.aip.org/aip/apl/article/103/15/152108/25270/Electron-hole-pair-generation-in-SiC-high
9 E. V. Kalinina, A. M. Ivanov, N. B. Strokan, and A. A. Lebedev: Semicond. Sci. Technol. **26** (2011) 045001. https://iopscience.iop.org/article/10.1088/0268-1242/26/4/045001
10 H. Nakagawa, K. Hayashi, A. Miyazawa, Y. Honda, H. Amano, T. Aoki, and T. Nakano: Sens. Mater. **36** (2024) 169. https://sensors.myu-group.co.jp/article.php?ss=4647

11 H. W. Hou, Z. Liu, J. H. Teng, T. Palacios, and S. J. Chua: Sci. Rep. **7** (2017) 46664. https://www.nature.com/articles/srep46664
12 S. F. Kozlov, R. Stuck, M. Hage-ali, and P. Sffert: IEEE Trans. Nucl. Sci., **NS-22** (1975) 160. https://ieeexplore.ieee.org/abstract/document/4327634
13 Y. Tanimura, J. Kaneko, M. Katagiri, Y. Ikeda, T. Nishitani, H. Takeuchi, and T. Iida: Nucl. Instrum. Methods Phys. Res., Sect. A **443** (2000) 325. https://www.sciencedirect.com/science/article/pii/S0168900299010487
14 A. Kumar, A. Kumar, A. Topkar, and D. Das: Nucl. Instrum. Methods Phys. Res., Sect. A **858** (2017) 12. https://www.sciencedirect.com/science/article/pii/S016890021730373X
15 C. Weiss, J. Wilson, G. Tiebel, P. Steinegger, E. Griesmayer, H. Frais-Kölbl, R. Dressler, M. Camarda, and M. del Mar Carulla Areste: Nucl. Instrum. Methods Phys. Res. Sect. A **1040** (2022) 167182. https://www.sciencedirect.com/science/article/pii/S0168900222005472
16 H. Sumiya, N. Toda, Y. Nishibayashi, and S. Satoh: J. Cryst. Growth **178** (1997) 485. https://www.sciencedirect.com/science/article/pii/S002202489600797X
17 H. Sumiya, N. Toda, and S. Satoh: J. Cryst. Growth, **237**–**239** (2002) 1281. https://www.sciencedirect.com/science/article/pii/S0022024801021455
18 M. Marchwka, P. E. Pehrsson, D. J. Vestyck Jr., and D. Mosas: Appl. Phys. Lett. **63** (1993) 3521. https://pubs.aip.org/aip/apl/article/63/25/3521/62498/Low-energy-ion-implantation-and-electrochemical
19 N. P. Parikh, J. D. Hunn, E. McGucken, M. L. Swanson, C. W. White, R. A. Rudder, D. P. Malta, J. B. Posthill, and R. J. Markunas: Appl. Phys. Lett. **61** (1992) 3124. https://pubs.aip.org/aip/apl/article/61/26/3124/524530/Single-crystal-diamond-plate-liftoff-achieved-by
20 Y. Mokuno, A. Chayahara, and H. Yamada: Diamond Relat. Mater. **17** (2008) 415. https://www.sciencedirect.com/science/article/pii/S0925963508000022
21 T. Shimaoka, J. H. Kaneko, M. Tsubota, H. Shimmyo, H. Watanabe, A. Chayahara, H. Umezawa, and S. Shikata, Europhys. Lett. **113** (2016) 62001. https://iopscience.iop.org/article/10.1209/0295-5075/113/62001/meta
22 T. Shimaoka, J. H. Kaneko, Y. Sato, M. Tsubota, H. Shimmyo, A. Chayahara, H. Watanabe, H. Umezawa, and Y. Mokuno: Phys. Status Solidi A **213** (2016) 2629. https://onlinelibrary.wiley.com/doi/full/10.1002/pssa.201600195
23 T. Shimaoka, J. H. Kaneko, K. Ohtani, M. Tsubota, H. Shimmyo, A. Chayahara, H. Umezawa, H. Watanabe, S. Shikata, M. Isobe, and M. Osakabe: Rev. Sci. Instrum. **87** (2016) 023503. https://pubs.aip.org/aip/rsi/article/87/2/023503/1021330/A-diamond-14-MeV-neutron-energy-spectrometer-with
24 T. Tachibana, B. E. Williams, and J. T. Glass: Phys. Rev. B **45** (1992) 11975. https://journals.aps.org/prb/abstract/10.1103/PhysRevB.45.11975
25 K. Hecht: Zeitschrift für Physik **77** (1932) 235. https://link.springer.com/article/10.1007/BF01338917
26 K. Ueda, K. Kawamoto, and H. Asano: Diamond Relat. Mater. **57** (2015) 28. https://www.sciencedirect.com/science/article/pii/S0925963515000448
27 P. John, N. Polwart, C. E. Troupe, and J. I. B. Wilson: Diamond Relat. Mater. **11** (2002) 861. https://www.sciencedirect.com/science/article/pii/S0925963501006732